Laser and Particle Beams (2013), *31*, 123–127.

doi:10.1017/S0263034612000997

Effect of inside diameter of tip on proton beam produced by intense laser pulse on double-layer cone targets

FENGJUAN WU,[1,2] WEIMIN ZHOU,[1] LIANQIANG SHAN,[1] ZONGQING ZHAO,[1] JINQING YU,[1] BO ZHANG,[1] YONGHONG YAN,[1] ZHIMENG ZHANG,[1] AND YUQIU GU[1]

[1]Science and Technology on Plasma Physics Laboratory, Research Center of Laser Fusion, China Academy of Engineering Physics, Mianyang, Sichuan, China
[2]Laboratory for Extreme Conditions Matter Properties, Southwest University of Science and Technology, Mianyang, Sichuan, China

(Received 24 August 2012; Accepted 7 October 2012)

Abstract

The laser-driven acceleration of proton beams from a double-layer cone target, comprised of a cone shaped high-Z material target with a low density proton layer, is investigated via two-dimensional fully relativistic electro-magnetic particle-in-cell simulations. The dependence of the inside diameter (ID) of the tip size of a double-layer cone target on proton beam characteristics is demonstrated. Our results show that the peak energy of proton beams significantly increases and the divergence angle decreases with decreasing ID size. This can be explained by the combined effects of a stronger laser field that is focused inside the cone target and a larger laser interaction area by reducing the ID size.

Keywords: Double-layer cone target; Inside diameter; Laser-plasma interaction; PIC simulation; Proton acceleration

INTRODUCTION

With the development of high power lasers, it has become possible to generate MeV proton beams in experiments (Kluge *et al.*, 2012; Gaillard *et al.*, 2011). The accelerated proton beams have potential applications in several fields, including hadron therapy (Fritzler *et al.*, 2003), proton beam-driven fast ignition (Roth *et al.*, 2001), injectors for conventional particle accelerators (Krushelnick *et al.*, 2000), etc. However, most of these applications demand ion beams of high quality, such as narrow energy spread, high energy, low beam divergence, etc. Efforts have been made to improve energy spectra, collimation, and laser-beam coupling (Morita *et al.*, 2008; Renard-Le Galloudec D'Humieres, 2010; Yu *et al.*, 2012; Zhou *et al.*, 2010).

For currently available laser intensities, the dominant mechanism for high energy ion acceleration in laser-plasma interaction is target normal sheath acceleration (TNSA) (Wilks *et al.*, 2001), in which protons on the rear side of target are accelerated by electrostatic field of fast electrons penetrating the rear surface and escaping into vacuum. Therefore, a critical challenge of the TNSA mechanism is to increase the efficiency of converting laser energy into hot electrons, which further set up an electrostatic field for proton acceleration.

Sentoku *et al.* (2004) found that hollow cone targets have high energy conversion efficiency from laser pulse to hot electrons via PIC simulation. After that, cone structure targets have been intensively investigated, e.g., flat-tip cone (Kluge *et al.*, 2012), cone-wire (Ma *et al.*, 2012), double cones (Cai *et al.*, 2009), conical nanobrush (Yu *et al.*, 2012), cone-funnel (Ban *et al.*, 2012), etc. However, these relatively complex targets are hard to fabricate. Recently, Zhou *et al.* (2010) demonstrated that higher energies and better collimation proton beams can be achieved using hollow and high-Z material cone shaped target coated with an additional sub-micron and relatively low density proton layer compared with plane target. In fact, there are mainly two effects in a cone target. The first one is the focusing of laser pulse inside the cone target (Sentoku *et al.*, 2004), and the second one is the interaction of the laser pulse with the cone walls to generate high energy electron current (Kluge *et al.*, 2012; Gaillard *et al.*, 2011). In this paper, we use the two-dimensional fully relativistic electro-magnetic particle-in-cell (PIC) code FLIPS2D to simulate the interactions between laser and hollow double-layer cone targets

Address correspondence and reprint requests to: Yuqiu Gu, Science and Technology on Plasma Physics Laboratory, Research Center of Laser Fusion, China Academy of Engineering Physics, Mianyang, Sichuan Province, 621900, China. E-mail: yqgu@ceap.ac.cn

and study how the inside diameter (ID) of the tip size of cone target influence the proton beam characteristics (e.g., energy spectrum and beam divergence).

PIC SIMULATIONS

The simulations have been performed using PIC code FLIPS2D (Zhou *et al.*, 2010). The code applies finite difference methods to solve the field equations, a Boris's method to solve the motion of particles (Birdsall Langdon, 1991), and charge conservation method of first-order algorithm to make the simulation faster (Umeda *et al.*, 2003). The simulation box volume $x \times y = 60\,\lambda \times 40\,\lambda$ is divided into 2400×1600 cells and the time step is 0.0125 τ, where λ = 1μm is the laser wavelength and τ is the laser period. Seven particles are used in one mesh, and the total number of particles is about 2×10^7. The boundary conditions of fields are reflected on the left hand boundary, and boundary conditions of particles are absorption and then reemission. A *p*-polarized Gaussian laser pulse propagates along the *x* axis from the left boundary, and transverse focal spot diameter is 6 λ full width at half maximum. The laser beam rises up in 5 τ, with a sinusoidal profile, after which it maintains its peak intensity for 20 τ, and then falls to zero in another 5 τ. The peak intensity $I_0 = 3.5 \times 10^{19}$ W/cm^2 , which corresponds to a normalized vector potential $a_0 = 5.0$.

Our target is shown in Figure 1. The width of the cone wall is 3 μm, the cone angle is 30° (the optimum cone opening angle for fast ignition (Nakamura *et al.*, 2007*b*) and the ID size varies from 0λ to 10λ. The electron density is $10n_{cr}$ in the main part of the target and is $1n_{cr}$ in the proton layer behind the rear surface of the cone substrate, where $n_{cr} = \omega^2 m_e/4\pi e^2$ is the critical density.

HOT ELECTRONS PRODUCTION AND SHEATH FIELD ON THE TARGET'S REAR SURFACE

From Poisson' equation, the accelerating electric field acting on the proton is $E_{accl} = T_e/e[max(L_n, \lambda_D)]$, where T_e is the hot electron temperature, L_n is the local scale length of the expanding plasma, and λ_D is the Debye length (Wilks *et al.*, 2001). The magnitude of the accelerating electric field E_{accl} depends on the temperature of the escaping hot electrons as well as on local Debye length in the plasma, which in turn depends on the plasma electron temperature and density.

Figure 2 shows the time-integrated energy spectrum of electrons (0.5–20 MeV) behind the rear side of cone target at $t = 50\tau$, and is fitted by a Maxwellian distribution. The hot electron temperatures are given by 4.1 MeV, 3.3 MeV, 3.0 MeV, and 0.8 MeV for cases ID = 0 λ, 3 λ, 6 λ and 10′λ, respectively. Total number of hot electrons passed through the rear side is almost the same, but the component of high energy electrons significantly increases with decreasing ID size.

Figure 3 shows the dependence of average hot electron energy (0.5–20 MeV) behind the rear side at the the initial locations in the cone target at $t = 50$ τ. We can see that the average hot electron energy at the same original location increases with decreasing the ID size. When we reduce the ID size, the interaction surface area of cone wall with laser pulse increases. Furthermore, the number of electrons extracted from the cone wall per wavelength is $N_e = (a_0\, n_c\, \lambda_L/\pi)$ sin θ (Sentoku & Downer, 2010). θ is the angle between the cone surface and the propagation direction of the incident laser light, and λ_L is the laser wavelength. With the decreasing of the ID size, the laser field is intensified inside the cone target (corresponding to an increase of a_0), and therefore the number of higher energy hot electrons extracted from the cone wall increases. These hot electrons from the cone wall can gain forward momentum via the $\mathbf{v} \times \mathbf{B}$ term of the Lorentz force or vacuum heating (Brunel, 1987), and then are guided along the surface toward the cone tip by the

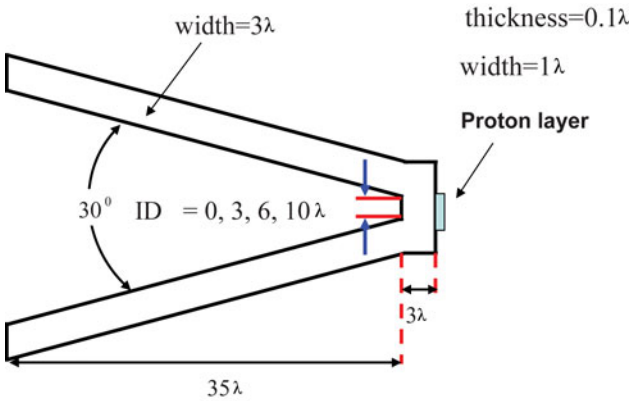

Fig. 1. Schematic diagram of cone-shaped substrate and the coated proton layer.

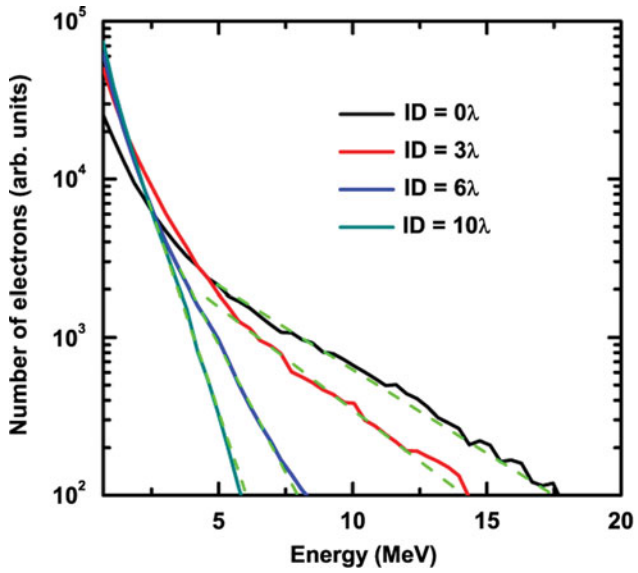

Fig. 2. Time-integrated energy spectrum of the hot electrons (0.5–20 MeV) observed at the rear side of the cone target for, respectively, a 0 λ 3 λ6 λ and 10 λ ID size of cone target at $t = 50$ τ.

https://doi.org/10.1017/S0263034612000997 Published online by Cambridge University Press

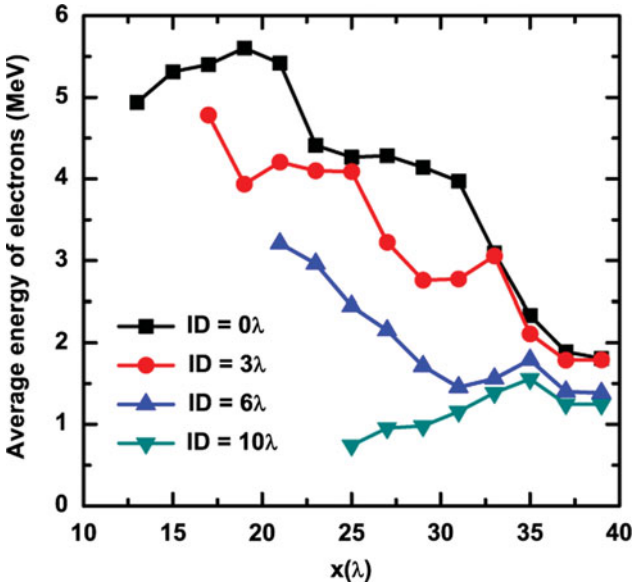

Fig. 3. The average hot electron energy (0.5–20 MeV) observed at the rear side of the cone target vs the original location in the cone target for, respectively, a 0 λ, 3 λ, 6 λ and 10 λ ID size of cone target at $t = 50$ τ.

strong self-generated quasistatic magnetic field. Subsequently, these hot electrons guided to the cone tip may be further accelerated by the ponderomotive force in the laser propagation direction (Nakamura *et al.*, 2007*a*). Meanwhile, the low energy components of hot electrons are mainly generated from the cone tip, and are accelerated by the ponderomotive force.

When these electrons propagate through the target and enter the rear vacuum, they generate a strong sheath field according to Ampere's law, $\partial \mathbf{E}/\partial t = -\mathbf{J}$. Since the protons are accelerated directly by the sheath field at the rear surface of the target in the TNSA mechanism, a comparison of the longitudinal electric field E_x (x, y) is shown in Figures 4 and 5.

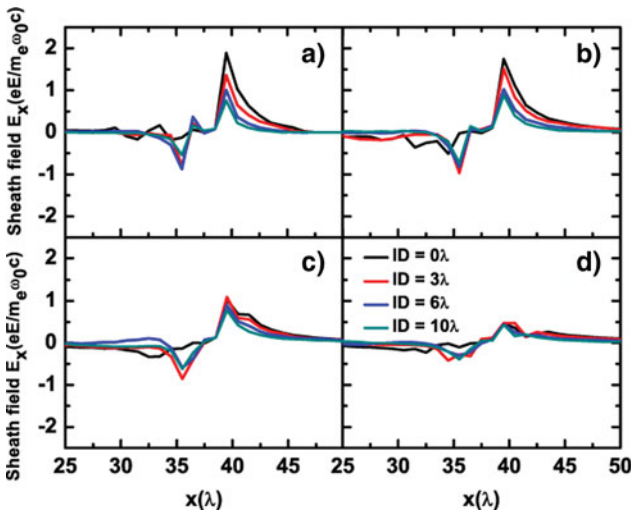

Fig. 4. The longitudinal sheath field E_x (x) (the cut is longitudinal on the propagation axis ($x = 0$)) for, respectively, a 0 λ, 3 λ, 6 λ and 10 λ ID size of cone target at $t =$ (**a**) 50 τ, (**b**) 60 τ, (**c**) 70 τ, (**d**) 80 τ.

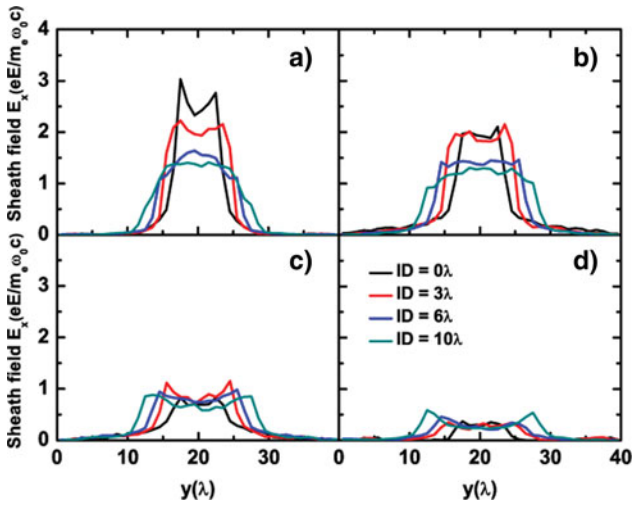

Fig. 5. The longitudinal sheath field E_x (y) (the transverse cut right at the vacuum-target interface ($x = 39$ μm)) for, respectively, a 0 λ, 3 λ, 6 λ and 10 λ ID size of cone target at $t =$ (**a**) 50 τ, (**b**) 60 τ, (**c**) 70 τ, (**d**) 80 τ.

From Figure 4, we find that E_x (x) shows an exponential decay in the longitudinal direction, because the amplitude of shield field on the rear surface is proportional to the temperature of hot electrons. As the ID size decreases, higher energy hot electrons expand faster into the vacuum, resulting in a higher amplitude and more broadly distribution of the electric field on the rear surface of the cone target. The stronger sheath field effectively accelerates the protons to higher energies.

Figure 5 shows that the transverse profile of longitudinal electricfield E_x (y), which determines the divergent properties of electrons, and therefore influences the divergence of the protons beams. With decreasing the ID size, the transverse width of E_x (y) is reduced and the strength of E_x (y) is increased, which leads to a smaller divergence angle of the proton beam. From above analysis, we find that the ID size of cone target can significantly influence the electron beam trajectory, and further affect the sheath field of the target rear surface.

DEPENDENCE OF PROTON YIELD ON ID SIZE OF THE CONE TARGET

The sheath field at the rear surface is responsible for the proton acceleration. In Figure 6, we show the time-integrated energy spectrum and angular distribution of proton emission observed from the cone targets and a plane target at $t =$ 100 τ. The emission angle $\phi = \arctan(v_y/v_x)$. For a plane target, the high-Z layer is 16 λ wide and 3 λ thick, and the low density proton layer is same as that in the cone target, i.e. 1 λ wide and 0.1 λ thick.

From Figure 6 we can see that the proton peak energy increases significantly and has a slightly decreasing divergence angle with decreasing ID size. For a plane target (dashed line), the proton peak energy is $E_{peak} = 3.4$ MeV, and the

https://doi.org/10.1017/S0263034612000997 Published online by Cambridge University Press

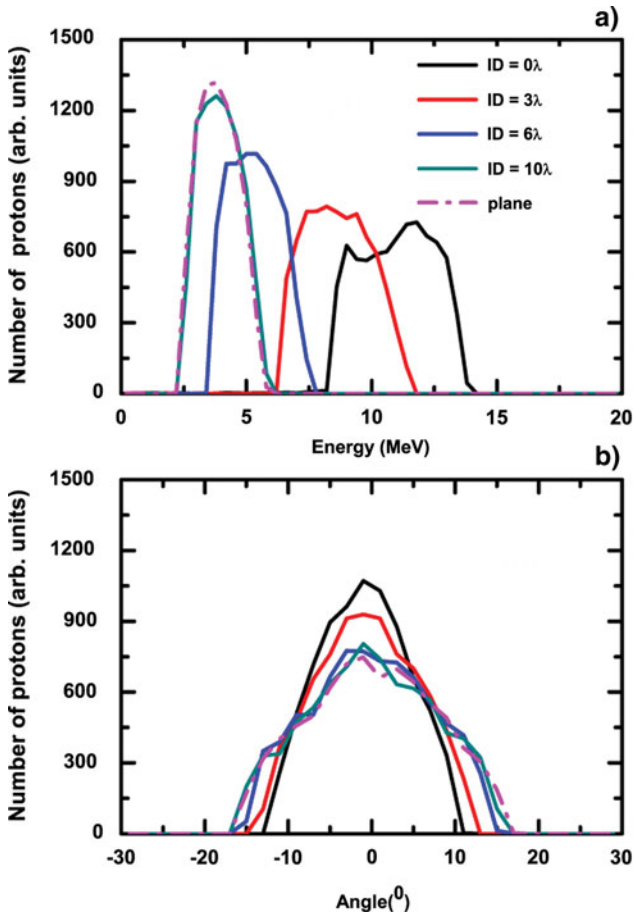

Fig. 6. Four cases of different ID sizes of cone targets and a plane target at $t = 100\ \tau$ (**a**) proton energy spectra, (**b**) proton emitted angle ϕ.

energy spread is $E_{FWHM}/E_{peak} = 73.5\ \%$. From Figure 6a, it can be seen that the peak energy ranges from 3.8 MeV to 11.8 MeV, for different ID sizes, and corresponding energy spread E_{FWHM}/E_{peak} ranges from 63.2% to 41.5%. For the case of an ID = 0 λ, the proton peak energy is approximately three times that using a plane target. In Figure 6b, as the ID size decreases, the emission angle ϕ_{FWHM} of the proton beam decreases from 23° to 15°, which can be attributed to the distribution of the longitudinal sheath field in the transverse direction for proton acceleration as shown in Figure 5.

CONCLUSIONS

In conclusion, we have performed FLIPS2D simulations to study how the ID size affects proton beams generated in double-layer cone target. For a fixed opening angle of cone target (30°), decreasing ID size can both enhance the laser focusing effects and increase laser interaction with the cone wall. The combined effects of a larger effective surface area and a further intensified laser field lead to higher coupling efficiency to hot electrons, which therefore result in a higher amplitude and more broadly distribution of the sheath field behind the rear surface of the cone target. As a result, a higher energy and narrower divergence angle proton beams are achieved by reducing the ID size of double-layer cone target. The result indicates that the case of ID = 0 λ cone target is favorable for accelerating higher energy and lower emission angle proton beams.

ACKNOWLEDGMENTS

We thank Prof. Dino Jaroszynski for helpful discussions. This work is supported by National Natural Science Foundation of China under Grant Nos 11174259, 11175165.

REFERENCES

Ban, H.Y., Gu, Y.J., Kong, Q., Li, Y.Y., Zhu, Z. & Kawata, S. (2012). Quasi-monoenergetic tens-of-MeV proton beams by a laser-illuminated funnel-like target. *Chin. Phys. Lett.* **29**, 035202.

Birdsall, C.K. & Langdon, A.B. (1991). *Plasma Physics Via Computer Simulation*. New York: McGraw-Hill.

Brunel, F. (1987). *Not-so-resonant, resonant absorption. Phys. Rev. Lett.* **59**, 52–55.

Cai, H.B., Mima, K., Zhou, W.M., Jozaki, T., Nagatomo, H., Sunahara, A. & Mason, R.J. (2009). Enhancing the number of high-energy electrons deposited to a compressed pellet via double cones in fast ignition. *Phys. Rev. Lett.* **102**, 245001.

Fritzler, S., Malka, V., Grillon, G., Rousseau, J.P., Burgy, F., Lefebvre, E., d'Humiéres, E., McKenna, P. & Ledingham, K.W.D. (2003). Proton beams generated with high-intensity lasers: Applications to medical isotope production. *Appl. Phys. Lett.* **83**, 3039–3041.

Gaillard, S.A., Kluge, T., Flippo, K.A., Bussmann, M., Gall, B., Lockard, T., Geissel, M., Offermann, D.T., Schollmeier, M., Sentoku, Y. & Cowan, T.E. (2011). Increased laser-accelerated proton energies via direct laser-light-pressure acceleration of electrons in microcone targets. *Phys. Plasma* **18**, 056710.

Kluge, T., Gaillard, S.A., Flippo, K.A., Burris-Mog, T., Enghardt, W., Gall, B., Geissel, M., Helm, A., Kraft, S.D., Lockard, T., Metzkes, J., Offermann, D.T., Schollmeier, M., Schramm, U., Zeil, K., Bussmann, M. & Cowan, T.E. (2012). High proton energies from cone targets: electron acceleration mechanisms. *NEW J. Phys.* **14**, 023038.

Krushelnick, K., Clark, E.L., Allott, R., Beg, F.N., Danson, C.N., Machacek, A., Malka, V., Najmudin, Z., Neely, D., Norreys, P.A., Salvati, M.R., Santala, M.I.K., Tatarakis, M., Watts, I., Zepf, M. & Dangor, A.E. (2000). Ultrahigh-intensity laser-produced plasmas as a compact heavy ion injection source. *IEEE Trans. Plasma Sci.* **28**, 1110–1115.

Ma, T., Sawada, H., Patel, P.K., Chen, C.D., Divol, L., Higginson, D.P., Kemp, A.J., Key, M.H., Larson, D.J., Le Pape, S., Link, A., MacPhee, A.G., McLean, H.S., Ping, Y., Stephens, R.B., Wilks, S.C. & Beg, F.N. (2012). Hot electron temperature and coupling efficiency scaling with prepulse for cone-guided fast ignition. *Phys. Rev. Lett.* **108**, 115004.

Morita, T., Esirkepov, T.Zh., Bulanov, S.V., Koga, J. & Yamagiwa, M. (2008). Tunable high-energy ion source via oblique laser pulse incident on a double-layer target. *Phys. Rev. Lett.* **100**, 145001.

https://doi.org/10.1017/S0263034612000997 Published online by Cambridge University Press

Nakamura, T., Mima, K., Sakagami, H. & Johzaki, T. (2007*a*). Electron surface acceleration on a solid capillary target inner wall irradiated with ultraintense laser pulses. *Phys. Plasma* **14**, 053112.

Nakamura, T., Sakagami, H., Johzaki, T., Nagatomo, H., Mima, K. & Koga, J. (2007*b*). Optimization of cone target geometry for fast ignition. *Phys. Plasma* **14**, 103105.

Renard-Le Galloudec, N. & D'Humieres, E. (2010). New micro-cones targets can efficiently produce higher energy and lower divergence particle beams. *Laser Part. Beams* **28**, 513–519.

Roth, M., Cowan, T.E., Key, M.H., Hatchett, S.P., Brown, C., Fountain, W., Johnson, J., Pennington, D.M., Snavely, R.A., Wilks, S.C., Yasuike, K., Ruhl, H., Pegoraro, F., Bulanov, S.V., Campbell, E.M., Perry, M.D. & Powell, H. (2001). Fast ignition by intense laser accelerated proton beams. *Phys. Rev. Lett.* **86**, 436–439.

Sentoku, Y., Mima, K., Ruhl, H., Toyama, Y., Kodama, R. & Cowan, T.E. (2004). Laser light and hot electron micro focusing using a conical target. *Phys. Plasma* **11**, 3083–3087.

Sentoku, Y. & Downer, M.C. (2010). Heat transport in solid target following relativistic laser{matter interaction. *Hi. Ener. Density Phys.* **6**, 268–273.

Umeda, T., Omura, Y., Tominaga, T. & Matsumoto, H. (2003). A new charge conservation method in electromagnetic particle-in-cell simulations. *Comp. Phys. Commun.* **156**, 73–85.

Wilks, S.C., Langdon, A.B., Cowan, T.E., Roth, M., Singh, M., Hatchett, S., Key, M.H., Pennington, D., MacKinnon, A. & Snavely, R.A. (2001). Energetic proton generation in ultra-{intense laser{solid interactions. *Phys. Plasma* **8**, 542–549.

Yu, J.Q., Zhou, W.M., Jin, X.L., Cao, L.H., Zhao, Z.Q., Hong, W., Li, B. & Gu, Y.Q. (2012). Improvement of proton energy in high-intensity laser-nanobrush target interactions. *Laser Part. Beams* **30**, 307–311.

Zhou, W.M., Gu, Y.Q., Hong, W., Cao, L.F., Zhao, Z.Q., Ding, Y.K., Zhang, B.H., Cai, H.B. & Mima, K. (2010). Enhancement of monoenergetic proton beams via cone substrate in high intensity laser pulse-double layer target interactions. *Laser Part. Beams* **28**, 585–590.

https://doi.org/10.1017/S0263034612000997 Published online by Cambridge University Press